

# HYLIFE-II: A MOLTEN-SALT INERTIAL FUSION ENERGY POWER PLANT DESIGN—FINAL REPORT

R. W. MOIR, R. L. BIERI, X. M. CHEN, T. J. DOLAN, M. A. HOFFMAN, P. A. HOUSE, R. L. LEBER, J. D. LEE, Y. T. LEE, J. C. LIU, G. R. LONGHURST, W. R. MEIER, P. F. PETERSON, R. W. PETZOLDT, V. E. SCHROCK, M. T. TOBIN, and W. H. WILLIAMS

Lawrence Livermore National Laboratory, P.O. Box 808  
Livermore, California, 94551

KEYWORDS: ICF power plant design, ICF chamber engineering, Flibe

Received April 9, 1993

Accepted for Publication July 14, 1993

*Enhanced safety and performance improvements have been made to the liquid-wall HYLIFE reactor, yielding the current HYLIFE-II conceptual design. Liquid lithium has been replaced with a neutronically thick array of flowing molten-salt jets ( $\text{Li}_2\text{BeF}_4$  or Flibe), which will not burn, has a low tritium solubility and inventory, and protects the chamber walls, giving a robust design with a 30-yr lifetime. The tritium inventory is 0.5 g in the molten salt and 140 g in the metal of the tube walls, where it is less easily released. The 5-MJ driver is a recirculating induction accelerator estimated to cost \$570 million (direct costs). Heavy-ion targets yield 350 MJ, six times per second, to produce 940 MW of electrical power for a cost of 6.5¢/kW·h. Both larger and smaller yields are possible with correspondingly*

*lower and higher pulse rates. When scaled up to 1934 MW(electric), the plant design has a calculated cost of electricity of 4.5¢/kW·h. The design did not take into account potential improved plant availability and lower operations and maintenance costs compared with conventional power plant experience, resulting from the liquid wall protection. Such improvements would directly lower the electricity cost figures. For example, if the availability can be raised from the conservatively assumed 75% to 85% and the annual cost of component replacement, operations, and maintenance can be reduced from 6% to 3% of direct cost, the cost of electricity would drop to 5.0 and 3.9¢/kW·h for 1- and 2-GW(electric) cases.*

## I. INTRODUCTION

The Inertial Confinement Fusion (ICF) Program at Lawrence Livermore National Laboratory (LLNL) has been developing microexplosions of deuterium- and tritium-filled capsules in the laboratory. A potential future application of ICF is an electricity-producing power plant. While lasers are used now for laboratory research, a power plant might focus heavy-ion beams onto a target to initiate a microexplosion at a higher electrical efficiency and with a more practical interface between the driver beams and the reactor.

For a practical power plant, a reaction chamber must contain the radiation and blast effects of these small explosions many times a second for the life of the plant, usually 30 yr. Fifteen years ago, LLNL researchers

devised a reaction chamber with a thick liquid lithium array of jets that are injected between the explosions and the chamber walls. The effective thickness of this lithium jet array was  $\sim 0.75$  m. This liquid serves to attenuate fast neutrons before they strike the chamber walls, lengthening the lifetime of components, and also serves to breed tritium fuel. The design was called HYLIFE, which stands for high-yield lithium-injection fusion energy.<sup>1</sup> The other meaning implied by the name HYLIFE is the long life of the reactor chamber and components. In contrast, the first walls of magnetic fusion plants must be replaced every few years because of neutron damage.

The idea of a thick flowing liquid blanket made of jets was first put forth by Burke et al.<sup>2</sup> and Seifritz and Naegele<sup>3</sup> in 1975, and the version carrying the name

HYLIFE was conceived by Monsler et al.<sup>4</sup> in 1978. An extensive series of analyses on the fluid dynamics and blast attenuation by the jets was carried out by Glenn.<sup>5</sup> His references are extensively cited by Blink et al.<sup>1</sup>

Recently, we redesigned HYLIFE, incorporating enhanced safety features and reexamining all the conceptual designs of the plant components. We strongly endorse the basic design principle of interposing a neutronically thick liquid layer between the microexplosion and the chamber walls. (For discussion purposes, the original design with lithium walls is referred to as HYLIFE-I herein.) The new design,<sup>6,7</sup> called HYLIFE-II, replaces the liquid lithium (because of its fire hazard and large tritium inventory) with the molten salt, Flibe, which eliminates the fire hazards associated with lithium. Our use of molten salt relies heavily on early work at Oak Ridge National Laboratory on the molten-salt reactor.<sup>8</sup> The original HYLIFE-I design was based on a target gain of 400 with a laser driver energy of 4.5 MJ, whereas a gain of 70 with a driver energy of 5 MJ is now considered more likely, based on a better projection of heavy-ion-beam target performance. (Gain is defined as the ratio of fusion energy out of a target to driver energy onto the target.) This lower estimated gain of 70 reduces the yield from 1800 to 350 MJ and increases the pulse rate from 1.5 to 6 Hz. The higher pulse rate of HYLIFE-II requires careful attention to clearing of debris and liquid splash from the heavy-ion-beam paths between pulses.

The emphasis for future design work should be on strategies to lower the estimated cost of electricity (COE) by, for example, use of lower cost drivers and increased plant size, as well as design work to lower the cost of all plant components. The calculated 6.5¢/kW·h COE from HYLIFE-II for a 1-GW(electric) power plant is close to that of future coal-fired plants (5.8¢/kW·h) but higher than that of future light water reactor (LWR) nuclear power plants (4.3¢/kW·h) (Ref. 9). Of the 6.5¢/kW·h, the driver contributes 2.3¢/kW·h. These costs are in 1990 dollars. At this stage, however, cost estimates for inertial fusion energy (IFE) power plants are considered highly preliminary. Further, just how much an IFE power plant can cost and still be acceptable and economically competitive in future years remains to be seen. Other factors (e.g., safety, nonproliferation, and environmental aspects) will reflect on the future desirability of IFE, in addition to cost.

We show that a practical power plant can be based on fusion microexplosions and that the plant design is sufficiently robust to last for 30 yr. By practical, we mean that the plant is built with present-day materials and construction techniques and is cost-effective. This paper focuses on the reactor portion of the IFE power plant. Driver and target factory designs developed by other workers are included for completeness and costing. The remainder of this paper describes the plant features, discusses safety aspects, and gives estimates of the COE.

## II. SYSTEM OVERVIEW

Figure 1 shows the HYLIFE-II power plant. A circular recirculating induction accelerator delivers energy to fusion targets, producing six microexplosions per second in the reaction chamber to produce ~1 GW of electrical power for the reference design.

### II.A. Chamber and Jet Array Design

Figure 2 shows the HYLIFE-II chamber designed to contain the microexplosion and the liquid Flibe blanket that will protect the first structural wall (FSW) from neutron and blast damage.

One way to achieve a high-pulse rate is to arrange for a short distance between the nozzles that inject the Flibe and the microexplosion and to oscillate the jet nozzles horizontally, as shown in Fig. 2 (more details are given in Ref. 10). As the pulse rate increases, the flow speed of the liquid out of the nozzles increases, and the oscillation frequency increases. A pocket is formed in the flow where a target is injected and the microexplosion occurs (see Fig. 3). Following a microexplosion, the resulting Flibe splash must be cleared away enough to allow target injection and ion beam propagation for the next shot. The oscillating motion of the incoming liquid sweeps away splashed liquid left over from the previous microexplosion and clears the region inside the pocket. We expect the beam path outside the oscillating flow region to be cleared by the drag from the venting vapor formed in the previous microexplosion, although this has not been well modeled. The slots between the liquid slabs shown in Fig. 3 permit the vapor produced by the microexplosion to vent rapidly. This minimizes the outward acceleration of these liquid slabs and reduces the liquid impact force on the chamber walls. The oscillating flows are discussed more fully in Ref. 11. Mechanical moving parts allow the nozzles to oscillate at 6 Hz through a motion of  $\pm 2.5$  deg or  $\pm 0.09$  m at the nozzle tips. Fatigue and vibration appear manageable, but more detailed design work is required.

The liquid blanket is subjected to forces associated with X-ray ablation, gas pressure (form drag), and shear (skin drag) that impart an outward radial motion toward the vessel wall. These contributions may be augmented further by the net effect of breakup following neutron-induced isochoric heating of the blanket. (Isochoric, constant-volume heating is the intense, instantaneous, volumetric heating that occurs as the fusion neutrons are absorbed in the liquid, generating internal pressures of hundreds of atmospheres.) Each of these phenomena is strongly dependent on the geometry of the blanket jets. Detailed studies of isochoric heating have been carried out.<sup>12-14</sup> These studies show that liquid tension is developed during relaxation of the high pressure induced by the neutron pulsed heating and that this tension is strongly peaked. Thus, fracturing of the liquid will tend to form new surfaces with shapes

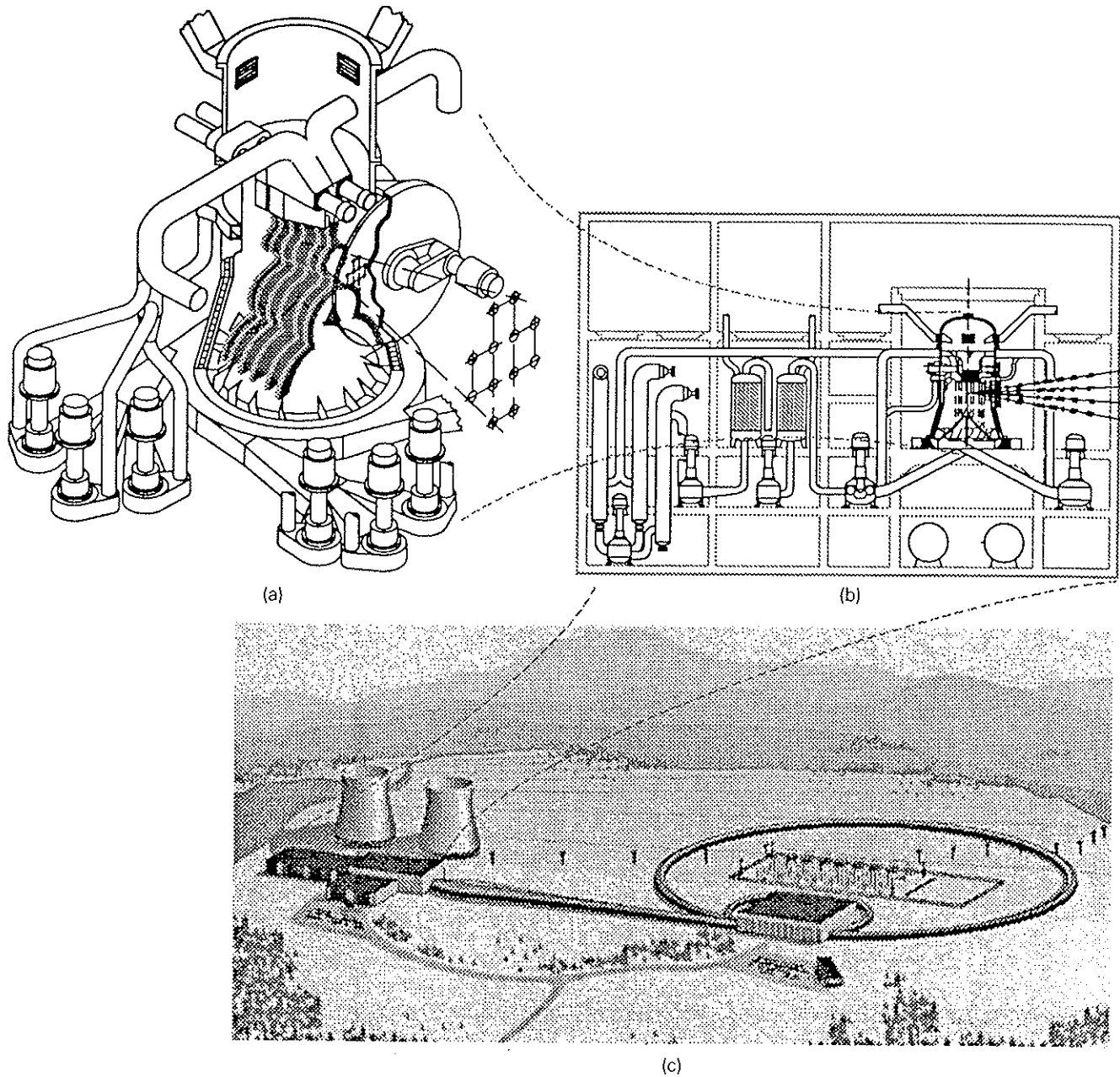


Fig. 1. HYLIFE-II, an IFE power plant design. A recirculating induction heavy-ion accelerator is used to ignite fusion micro-explosions six times per second to produce 1 GW of electrical power.

similar to the geometry of the blanket. HYLIFE-I used an array of 20-cm-diam cylindrical jets to form the falling lithium curtain. For that design, the jets would break in cylindrical surfaces with the outer annulus in outward motion. These moving annuli would impact against each other to largely cancel the individual, high-velocity motions of the slab pieces. Nevertheless, the radial gradient of neutron heating across the array would result in a significant net outward momentum with respect to the vessel radius. For the slab jet geometry adopted in the current design, the slabs will tend

to split along their axes from the end closest to the micro-explosion. A study<sup>6</sup> indicates that this form of fracture may cause some "jetting" of liquid parallel to the slabs and away from the central cavity as the broken ends collide. This would produce an asymmetric motion of the liquid toward the vessel wall. Detailed analysis of this effect remains to be done. However, our work indicates that less liquid motion toward the vessel wall will occur for slab jets than for cylindrical jets.

Detailed analysis of the central cavity gas dynamics has been carried out by Chen et al.<sup>15</sup> This analysis

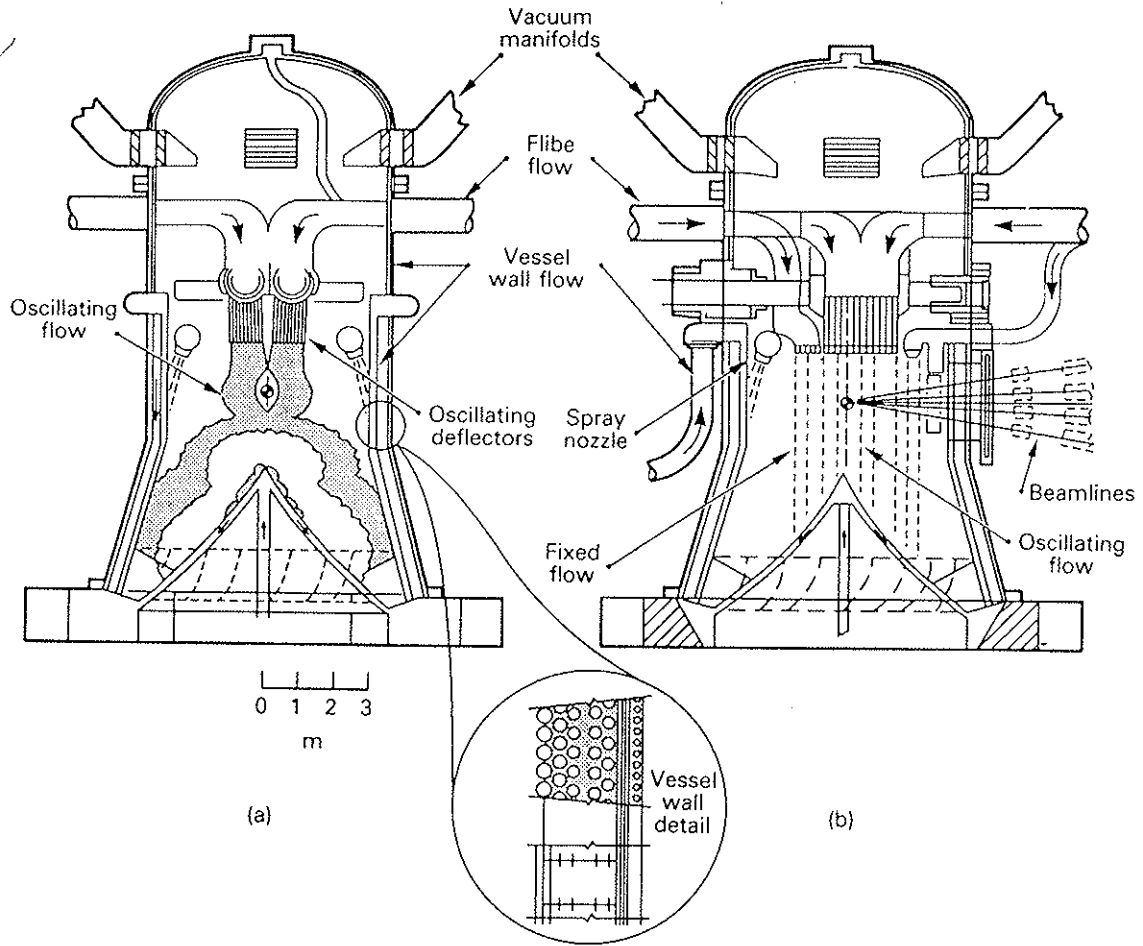


Fig. 2. HYLIFE-II reaction chamber. Liquid Flibe, formed into a "pocket" (i.e., the central cavity in the jet array) by oscillating nozzles, protects the chamber walls. View (b) is rotated 90 deg from view (a).

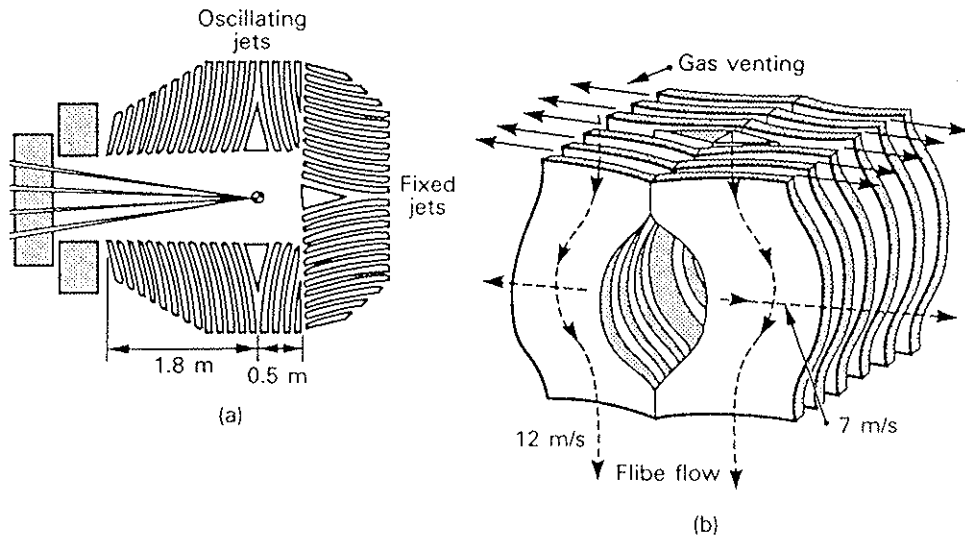


Fig. 3. The oscillating and stationary jets form a pocket that attenuates neutrons but vents vapor rapidly through the space between the liquid sheets or slabs.

gives an upper bound on liquid outward momentum caused by ablation from an idealized model of the blanket surface. The calculated contribution from this ablation is small, and the actual contribution for the slab jet geometries would be smaller still. Liu et al.<sup>16</sup> studied the gas venting problem for both cylindrical and slab jet geometries, with typical results illustrated in Fig. 4. Because the heat and mass transfer have been neglected, the results tend to overestimate the momentum imparted by form and viscous drag. Form drag is by far the major factor determining the liquid momentum. It has been shown that the form drag on the last row of jets in an array of cylindrical jets would be very large compared with those in the interior. This indicates a strong advantage for the slab jet design, which has a relatively low form drag per unit mass of jet. The results of this study also show that the venting forces are rather asymmetric with respect to the vessel axis not only for the slab design, but even for the cylindrical jet array design.

Considering all these interactions, we estimate that the blanket of the current design will receive an average outward velocity of  $\sim 7$  m/s, which would result in the liquid impacting the wall near the bottom of the vessel (Figs. 2 and 3) with an impact pressure of only 25 kPa. Given the complex nature of these phenomena, however, especially the rather unusual effect of isochoric heating, much more work needs to be done to predict the liquid motion with confidence.

## II.B. Plant Parameters

Table I shows the plant parameters for the 1-GW(electric) reference case<sup>17</sup> and for an enhanced power case of 2 GW(electric). Figure 5 shows the various power flows. The 2-GW(electric) case is interesting because it has a lower COE as is discussed later. The 5-MJ driver energy and 6-Hz pulse rate [to give  $\sim 1$  GW(electric)] were chosen somewhat arbitrarily, and future analysis of driver cost scaling and other technical features might change the preferred pulse rate. But the COE will probably not change much. Fixed-power, heavy-ion-driven IFE power plants have COEs that depend weakly on pulse rate near the minimum COE. Variations from the base OSIRIS design,<sup>18</sup> for example, gave a 5% decrease in COE when the pulse rate changed from 4.6 to 8.6 Hz.

For the higher driver energy of the enhanced case of 6.7 MJ, the target gain increases to  $\sim 90$ , as shown in Table I. This variation of target gain with driver energy is explained later.

## II.C. Plant Components

Figure 6 shows the plant components, up to the point where steam is generated for use in a conventional power plant, while Fig. 7 shows components for the balance of plant<sup>19</sup> (BOP). The temperature of the

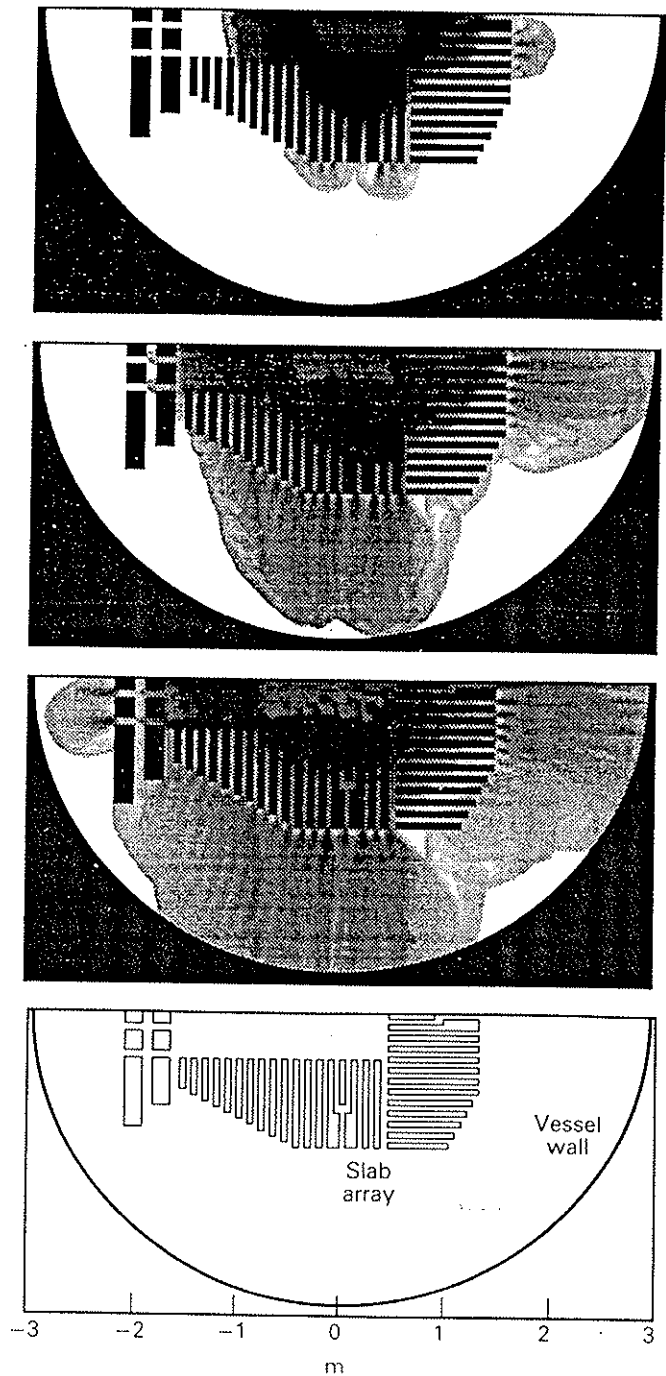


Fig. 4. Computed blast venting through liquid blanket in the HYLIFE-II ICF reactor shown at  $90\text{-}\mu\text{s}$  intervals. One-half of the reactor cavity is simulated by the Transient Shockwave Upwind Numerical Analysis Method for ICF (TSUNAMI) code. Nodalization is by a  $300 \times 600$  uniform Cartesian grid with 37 slab jets.

Fluibe is 923 K ( $650^\circ\text{C}$ ) entering the steam generators and 873 K ( $600^\circ\text{C}$ ) leaving. The layouts in Figs. 7 and 8 are for a version of HYLIFE-II that employs a subcritical steam cycle. The most recent version of HYLIFE-II

TABLE I  
Nominal Plant Parameters

	Reference Case: 1 GW(electric)	Enhanced Power Case: 2 GW(electric)
Driver energy (MJ)	5	6.7
Target gain	70	90
Yield (MJ)	350	600
Energy multiplication	1.18	1.18
Repetition rate (Hz)	6	7
Fusion power (MW)	2100	4220
Thermal power	2500	5000
Thermal efficiency (%)	43.0	43.0
Availability (%)	75.0	75.0
Gross electrical power (MW)	1075	2150
Recirculating power [MW(electric)]	135	216
Bypass pumping power (Flibe)	32	46
Driver input power	85	134
Other pumping power <sup>a</sup>	18	36
Net electricity power [MW(electric)]	940	1934

<sup>a</sup>Includes pumping power in the heat transport system and in the steam generator.

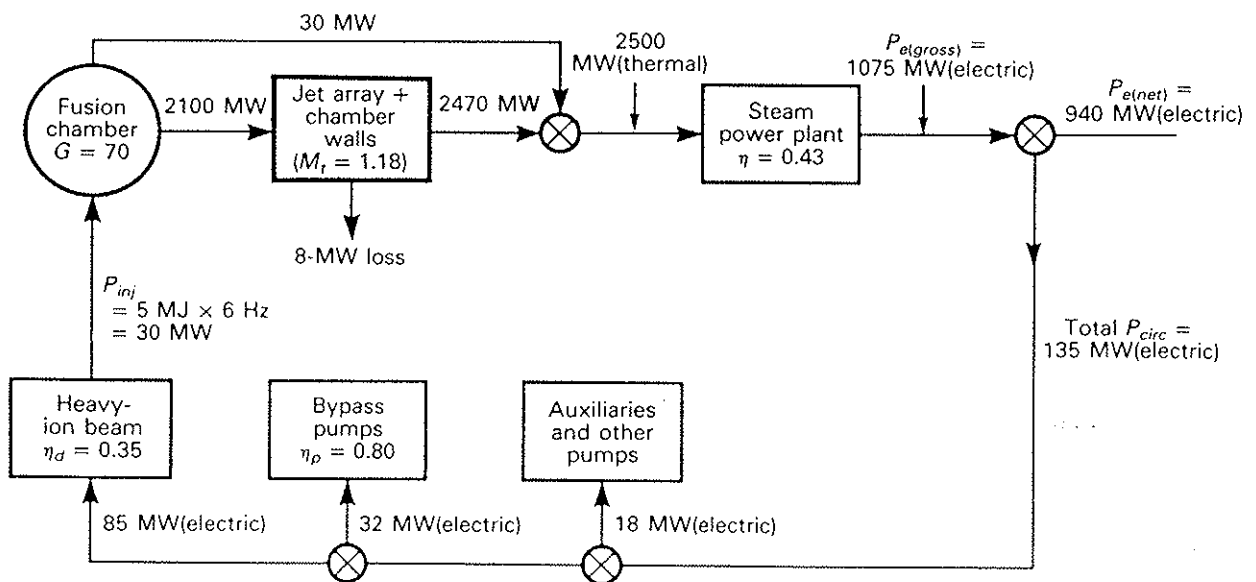


Fig. 5. The power flow diagram for the 940-MW(electric) reference case [referred to as the nominal 1-GW(electric) case in the text].

employs an advanced supercritical steam cycle with improved efficiency of  $\sim 43\%$ . Its layout will be very similar. The steam generators have double-walled tubes, which were chosen for increased reliability. The double-walled tubes only slightly decrease tritium migration into the steam since the greatest transport resistance is across the Flibe film at the tube walls.

#### II.D. Tritium Systems

Practically all of the unburned tritium gas emitted by exploding targets will be removed by the vacuum pumps on the reactor chamber. To be conservative, however, we assume that almost none of the tritium produced in the Flibe by neutron reactions with lithium

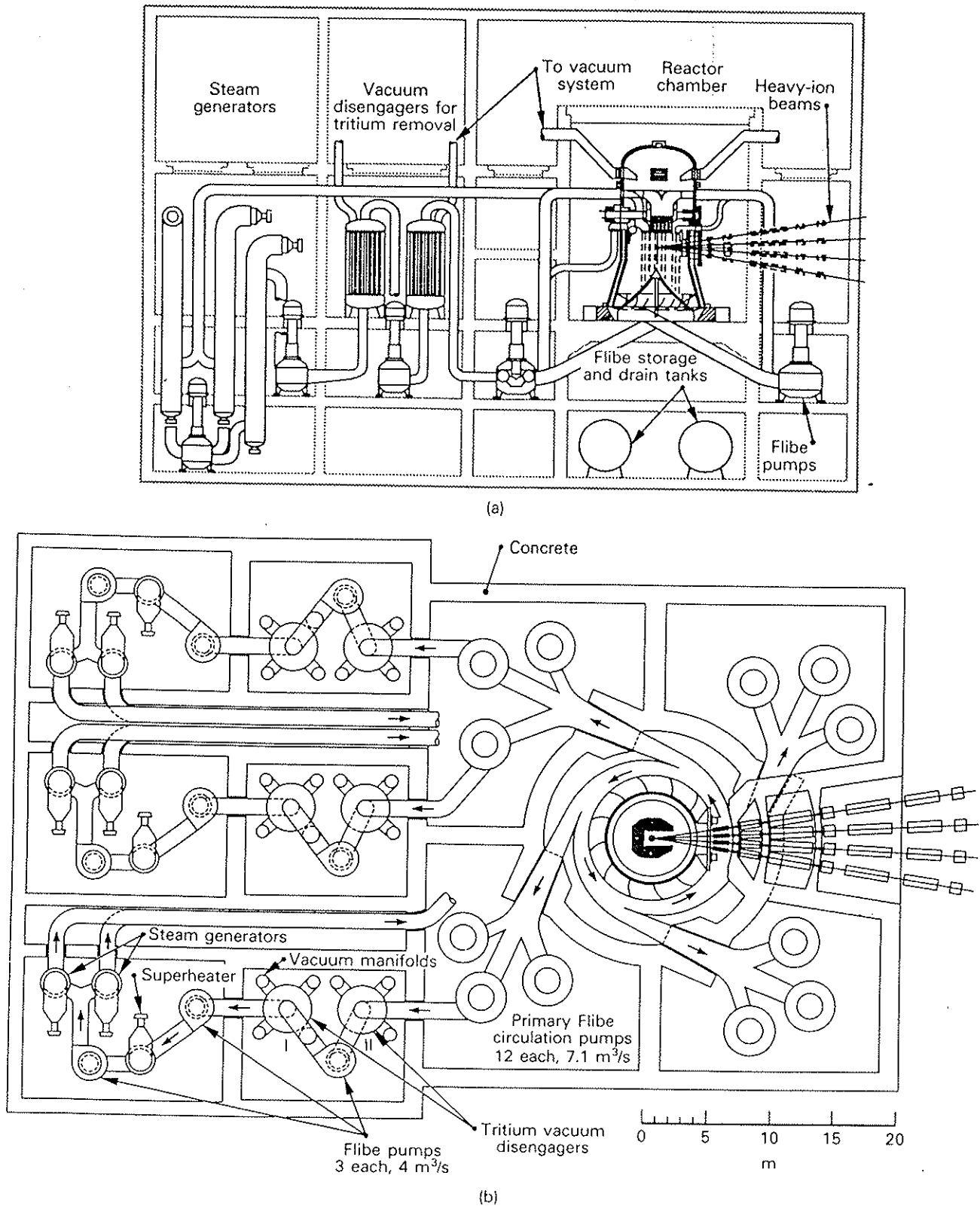


Fig. 6. Flibe heat transport components in a HYLIFE-II power plant with a subcritical steam cycle: (a) elevation view and (b) plan view. Effective tritium removal permits going from Flibe to steam without an intermediate loop. The steam generator is double-walled to minimize water leakage into the radioactive Flibe. A purge flow of helium gas between the double-walled piping from the reactor to the outlet of the vacuum disengager provides for the removal of the tritium that diffuses through the inner pipe wall.





$2.5 \times 10^6$  kg) of Flibe is a remarkably low 0.5 g because of its low solubility in Flibe. The estimated inventory in the metal walls of the chamber and piping is 140 g, which if released in an accident, would give an off-site dose of 13 mSv (1.3 rem). We have assumed 5 mSv (0.5 rem) as a working limit before nuclear certification is required<sup>22</sup>; however, this figure may be overly stringent (25 rem has been used in the nuclear industry). Because the estimated inventory exceeds 5 mSv, nuclear-grade components were chosen for the vacuum disengager, piping, and chamber. They could be avoided if the inventory were reduced by a factor of only 3 (see further discussion in Sec. V) or if a less restrictive criterion were assumed. The tritium in the processing system is estimated at 300 g. There is estimated to be a 1-day supply of tritium, 900 g, in the storage system and target factory, which are external to the reactor building. As a result, this tritium is not likely to be released by a reactor accident such as a pipe break. The total tritium inventory is estimated at 1.4 kg.

### II.E. Flibe Compared with Liquid Lithium

Either Flibe (HYLIFE-II) or liquid lithium (HYLIFE-I) can protect the components from neutron damage to make them last the life of the plant. A quantitative discussion of this point is given in Sec. III.

The lithium fire hazard in HYLIFE-I will be eliminated by using the low-viscosity molten salt, Flibe. It is compatible with Type 316 stainless steel or, even better, with Hastelloy N at a much higher temperature than lithium (923 compared with 770 K) because it does not have lithium's corrosion properties.<sup>23</sup> Because of the high melting point, care will be needed to prevent damage from the abnormal condition of freezing. This will be especially important in the steam generator. Its heat transfer properties, while not as good as those of lithium, are still sufficient to remove heat adequately. Unlike lithium, Flibe vapor partially dissociates from the X-ray and debris energy deposition but recombines again essentially completely and rapidly enough to not adversely affect condensation rates or limit the pulse rate.<sup>24</sup>

The inventory of Flibe in HYLIFE-II is 2500 tonnes ( $2.5 \times 10^6$  kg) of which 230 tonnes is beryllium. The resource of beryllium in the United States is 150 000 tonnes, which is sufficient to provide the beryllium in Flibe for 650 HYLIFE-II power plants.<sup>25</sup> The current U.S. beryllium production rate is sufficient to start up one plant per year; this production rate could easily be doubled or tripled if needed because the industry is well below capacity.

### II.F. Target Design Considerations

The target is designed for heavy ions such as  $^{200}\text{Hg}^{+}$  at 10 GeV. The gain depends on the energy delivered to the target, the beam radius (2 mm on the target), and the ion range in the target material ( $0.1 \text{ g/cm}^2$ ). Fig-

ure 9 shows the target gain curves for a 0-deg beam half-angle.<sup>26</sup> The beam half-angle is the angle encompassing the array of beams (12 in our case), as shown in Fig. 10. If the beam half-angle is  $\pm 9$  deg, as calculated for this design, we predict the gain will drop by  $\sim 16\%$  (see Fig. 2b of Ref. 27). To obtain a yield of 350 MJ with this 16% gain degradation will require raising the input energy to  $\sim 6$  MJ (as can be calculated from Fig. 9 for a range of  $0.1 \text{ g/cm}^2$  and a 2-mm focal spot size). The correction for beam angles leading to the 6-MJ driver for the 1-GW (electric) plant was not incorporated in the rest of this work, however, and a gain of 70 at 5 MJ is assumed.

The time dependence of the beam energy delivered to the target, called pulse shape, is obtained by time compressing the beam in the 400-m-long drift/compression section and by using the difference in arrival time due to the 3-m difference in path length shown in Fig. 9 (i.e., the beams can be compressed and stacked).

The two-sided target will be modified for illumination from one side (see Fig. 11). The modification involves rotating the beams by 90 deg so they come in from right to left. We assume the gain characteristics will be close to those of Fig. 9.

The target materials (Table II) were selected, based on discussions with Bangertter et al.<sup>28</sup> We chose tantalum for use in the target because of its relatively high  $Z$  ( $Z = 73$ ) and its solubility in Flibe as  $\text{TaF}_5$ . We can make coatings by chemical vapor or liquid deposition. The results of an activation analysis of tantalum are given by Tobin.<sup>29</sup> Many other high- $Z$  materials, such as lead and tungsten, would precipitate on the walls of the vessel and pipes, making recovery difficult and possibly causing other problems. Mercury might be acceptable if the vapor pressure could be kept low enough for beam propagation but high enough for recovery by the volatility (or distillation) process. The  $\text{TaF}_5$  could be recovered by distillation in the vacuum disengagers or by reaction with beryllium.

TABLE II

Target Materials and Blanket-Produced Materials for a Single Shot with a 350-MJ Yield Target (mass in milligrams)

	Target Before Shot	Target After Shot	Produced in Flibe
Lithium <sup>a</sup>	51	51	0
Tantalum <sup>b</sup>	220	220	0
Deuterium	1.2	0.79	0
Tritium	1.8	1.2	0.75
Helium	0	0.85	0.99

<sup>a</sup>Assuming lithium replaces the plastic ablator.

<sup>b</sup>Assuming tantalum is equally as effective as lead or mercury.

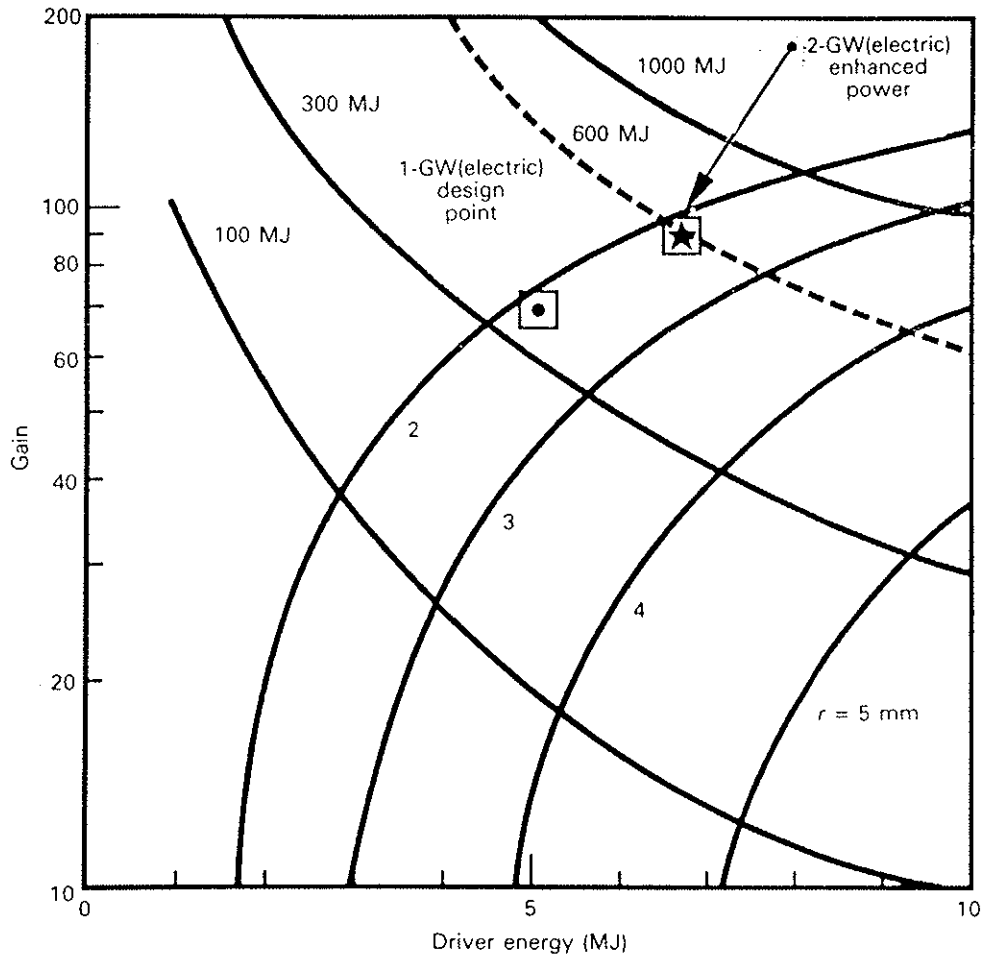


Fig. 9. Target gain as a function of driver energy for 0-deg beam half-angle. The radius  $r$  of the beam spot size is given as a parameter. The nominal design point is 5 MJ, gain 70 (just below that shown above), range  $0.1 \text{ g/cm}^2$ , and spot radius 2 mm. The actual beam half-angle of about  $\pm 9 \text{ deg}$  will lower the gain somewhat below the 2-mm spot size curve. Increasing the driver energy to  $\sim 6.7 \text{ MJ}$  will give a yield of 600 MJ for the 2-GW(electric) case.

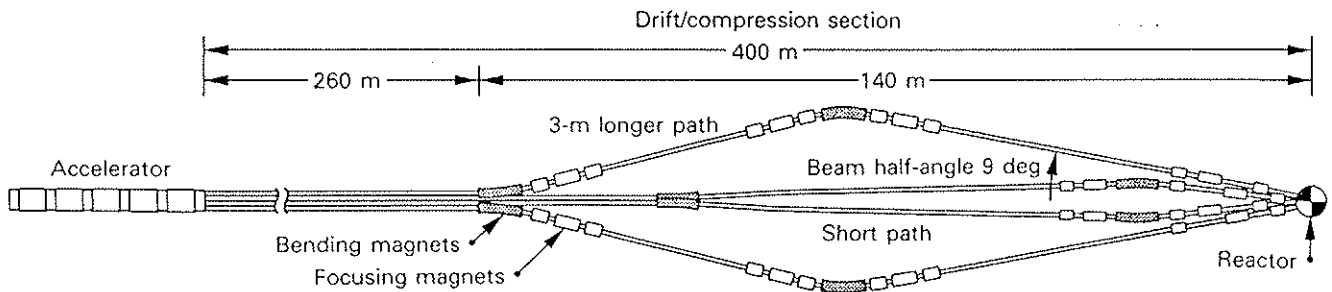


Fig. 10. Preliminary design of the final beam transport system for HYLIFE-II shows a 12-beam cluster within  $\pm 9 \text{ deg}$  for one-sided illumination.

A helium gas gun is proposed to inject targets into the chamber. At 100 m/s, the target takes 30 ms of the 167-ms interpulse time (6 Hz) to pass to the center of the 3-m-radius chamber. Target acceleration of 1000

$\text{m/s}^2$  (100 g) to 100 m/s takes 100 ms and requires a 5-m-long gun barrel. About 10 mg of compressed helium is required to inject each target, and the gas is differentially pumped to minimize entry into the reactor

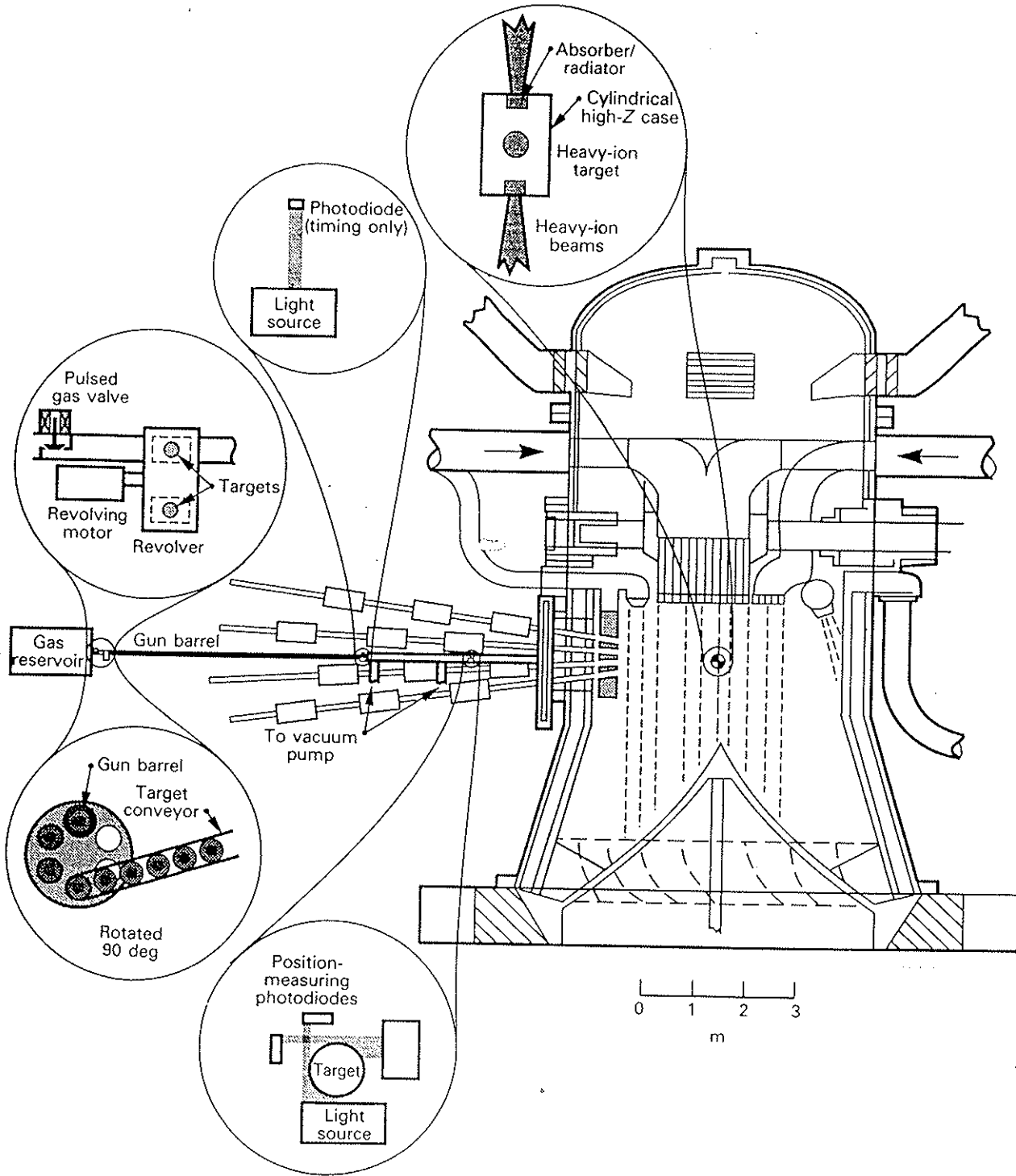


Fig. 11. The targets are injected with a gas gun and tracked with light beams. Either the double-ended targets must be re-designed to allow one-sided illumination or the beams must be directed from two sides.

chamber. (This pumping, along with the low  $Z$  of the gas, should minimize the effect this gas has on ion beam propagation.) As indicated in Figs. 11 and 12, the targets are injected horizontally into the pocket of the

Flibe jet array through the centerline of the driver beam cluster. The muzzle end of the injector is placed  $\sim 7$  m from the chamber center to allow room for tracking the target. Crossed light beams and photodetectors are

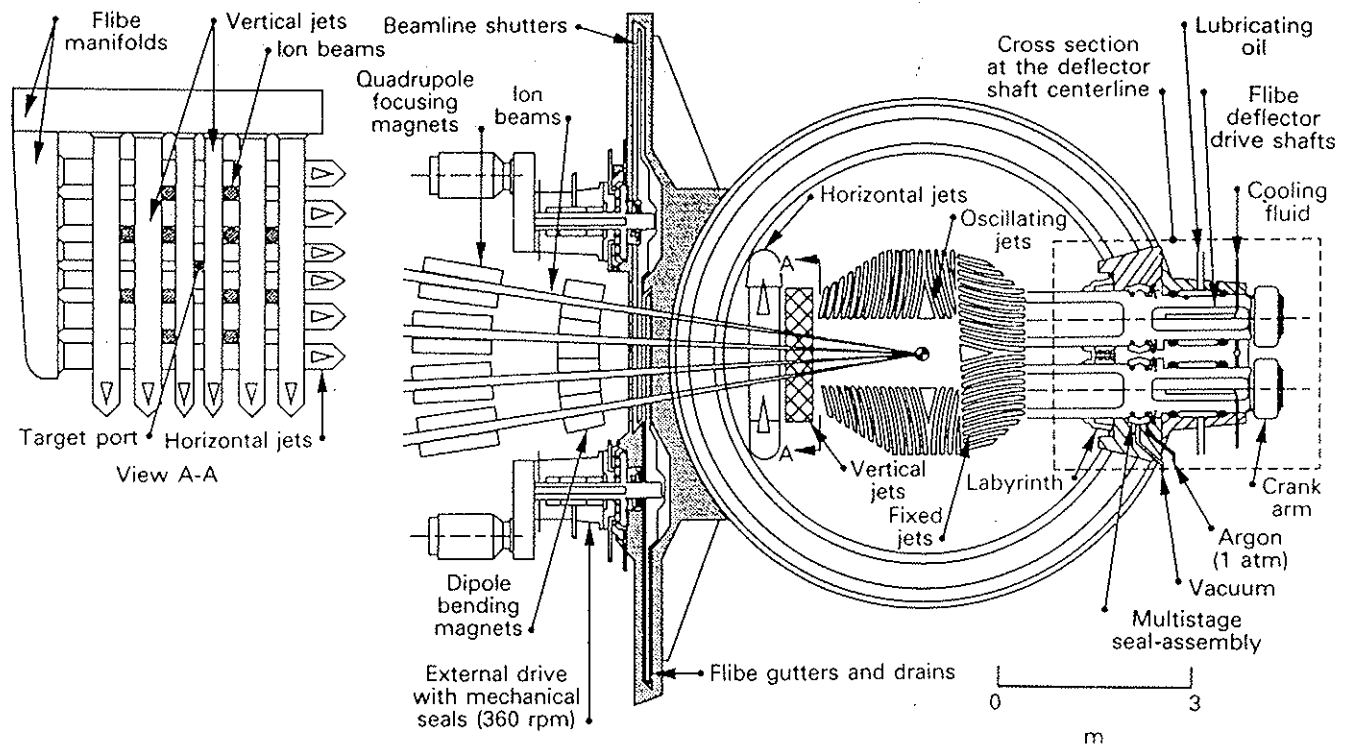


Fig. 12. Thick horizontal and vertical liquid jets protect the beam ports from radiation and help clear splashed liquid for the next shot. Rotating shutters help keep the beamlines clear of vapor and debris.

proposed to track the targets prior to entering the chamber. Target trajectory calculations are made, and information is fed to each of the 12 heavy-ion beams for pointing instructions so the beams will hit the target with sufficient accuracy. The required accuracy for driver beams on target is assumed to be  $\pm 0.4$  mm, which is 20% of the assumed 2-mm-radius driver beam spot size. This  $\pm 0.4$  mm will be the sum of the inaccuracies in target injection, in target tracking, and in beam pointing. Further study is required to ensure that this requirement can be met or exceeded.

For costing purposes, a target factory design by Woodworth<sup>30</sup> with a cost of about \$50 million was adopted.

### II.G. Driver and Repetition Rate Issues

Because this study focused on the reactor design, driver designs developed by others were considered, including a linear induction accelerator, a recirculating accelerator, a compact torus driver, and a laser driver.

Early estimates for a 5-MJ linear induction heavy-ion driver were based on preliminary designs and cost scaling used in the Heavy-Ion Fusion Systems Assessment study.<sup>31</sup> The chosen driver assumed  $^{200}\text{Hg}^+$  ions at 10 GeV and had an estimated direct cost of \$1.3 billion.<sup>32</sup> A more recent study<sup>33</sup> greatly reduced the estimated costs of a heavy-ion driver by using compact, high-performance ( $\text{Nb}_3\text{Sn}$ ) quadrupole arrays and ex-

amining a wide range of possible driver parameters. The resulting base 5-MJ driver uses 12 beams of  $^{131}\text{Xe}^+$  ions at 3.83 GeV and has a predicted cost of approximately \$600 million.<sup>18,33</sup> A recirculating induction accelerator has been designed with fewer acceleration cells for a given ion energy<sup>34</sup> with a predicted cost of \$500 million for 4 MJ and 35% efficiency. At 5 MJ, we scale the cost to \$570 million, assuming 0.6 power scaling.

Compact tori that are accelerated and focused require a much different target and transport system design<sup>35</sup> and are interesting because of their potentially lower cost (between \$100 and \$200 million).<sup>36</sup> However, these systems are speculative because the parameters required of compact torus accelerators are orders of magnitude beyond what is currently attained in laboratory experiments.

Laser drivers have been considered for HYLIFE-II (Ref. 6) but are not leading candidates at this time because of the combination of illumination geometry requirements for high gain, high cost, and low efficiency with the current understanding of target design. The HYLIFE-II illumination geometry makes laser direct drive and light-ion drive inappropriate. While lasers do not appear to be a good driver for HYLIFE-II currently, future developments in both target design and lasers may change this conclusion.

The driver selected for this study is the recirculating induction accelerator (Fig. 1). The choice between

a recirculating and linear machine would have no effect on the reactor design, however. With the current extensive research in heavy-ion drivers, future studies will determine the driver of choice for IFE power production.

Given the large cost of the driver, it may also be possible to cut the driver's contribution to the COE by having one driver switch to up to four reactors, each of 1-GW(electric) size, as was suggested in the HIBALL-II study.<sup>37</sup> Alternatively, a more modest suggestion is to increase the power in one chamber to 2 GW(electric), as shown in Table I, by increasing the driver energy to 6.7 MJ, which increases the yield to 600 MJ.

## II.H. Driver Interface Issues

Because the energy in a single beam is limited by space charge and emittance, 12 separate beams will provide the nominal 5-MJ total energy. Based on studies that considered arrays of 4, 12, and 24 beams, the 12-beam array is the most cost-effective.<sup>33</sup> The beams can be directed from two sides of the reactor or from only one side. Neutron and gamma-ray shielding must be added between the beam and the final focusing magnets to protect them from radiation damage. The shielding increases the magnet radius and will make it difficult to get a compact array of beams. The final transport system for the beams (Fig. 10) is from a study<sup>38</sup> done in 1990.

## II.I. Jet Design, Clearing, and Condensation

Several issues must be considered in the reactor design to allow 6-Hz operation. Of particular importance is the ability for Flibe splash from each pulse to be cleared from the beam path prior to the next pulse. It is also critical that enough condensation of vaporized Flibe in each pulse takes place to allow ion beam propagation through the chamber.

Continuously flowing, horizontal and vertical, neutrally thick liquid jets (shown in Fig. 12) will protect the beam ports from radiation damage. For gravity clearing of the beam paths through these jets, the vertical spacing between them should be  $< S$ , the distance initially stationary splash can fall between shots ( $S = 0.5gt^2$ ). For 6 Hz,  $S = 13.7$  cm. HYLIFE-II has a jet spacing of  $\sim 15$  cm. If the splash starts with an upward velocity, the distance  $S$  must be cut by up to a factor of 4. The vapor rushing outward may greatly assist in clearing liquid droplets from the beam paths. We must await experiments to determine the full extent of splash-clearing design problems.

Initially,  $\sim 16\%$  of the 350-MJ microexplosion yield is deposited by X-ray absorption in a thin layer on the exposed surfaces of the Flibe blanket, causing ablation (vaporization, dissociation, and ionization) of a small amount of mass. The vaporized material rapidly cools while expanding into the central cavity with high inward

velocity. It then interacts with the target debris (which carries an additional 16% of the yield) and recompresses [which increases its temperature again near the center of the chamber (or center of the pocket of Fig. 3)]. While at a temperature of 1 eV or more, the gaseous material radiates additional energy to the Flibe surfaces, causing further vaporization.<sup>15</sup> After reexpansion, the vapor impinges on and vents through the blanket within  $\sim 1$  ms (Ref. 16). Some condensation on the blanket surfaces is expected. The available surface area is, however, too small to produce sufficiently rapid condensation to restore the required vacuum (particle density in the range  $3 \times 10^{12}$  to  $3 \times 10^{13}$   $\text{cm}^{-3}$ ), for heavy-ion propagation for the next shot, within the allowed 0.167 s for 6-Hz pulse rate.<sup>38,39</sup> The physics of the interactions of venting vapor with Flibe jets will require additional analysis before the detailed assessment is complete.

For the current design, a conservative approach has been taken. Cold Flibe (much cooler than the bulk but still molten) will be sprayed into the annular region between the Flibe blanket and the vessel wall at a rate that is capable of condensing all the vapor, i.e., with no credit for condensation on the liquid jet blanket surfaces. Stated another way, it is assumed that the spray must absorb all the X-ray and debris energy (112 MJ). A method was developed by Bai and Schrock<sup>40</sup> to analyze the transient condensation on the spray. The analysis shows that heat diffusion within the Flibe is slow, such that the thermal penetration thickness is on the order of 0.3 mm in 0.17 s. A surface layer of the individual drop is first heated by the condensing vapor, but then, in a time shorter than the interpulse time, the drop becomes a vaporization source because of the rapidly falling vapor pressure (saturation temperature). The net condensation rate is the difference between condensation on the surfaces of newly injected drops and evaporation from the surfaces of the older drops.

A study of spray performance<sup>41</sup> led to the design selection of 2-mm-diam drops sprayed at a temperature of 843 K (50 K lower than the 893 K corresponding to a vapor density of  $3 \times 10^{13}$   $\text{cm}^{-3}$ ) and a flow rate of  $2.4 \times 10^3$  kg/s. This flow rate is only 1.6% of the main Flibe flow rate of  $150 \times 10^3$  kg/s (Ref. 10). It will require  $\sim 1$  MW of pumping power.<sup>41</sup> The spray will be provided by 205 spray heads  $\sim 10$  cm in diameter with seventeen hundred 1-mm-diam holes in each head. The location of the spray nozzle heads is shown in Fig. 2. The spray is directed such that the average length of drop trajectories is 1 m. Detailed calculations have not been done on the venting of the vapor through the droplets.

If the lower vapor density of  $3 \times 10^{12}$   $\text{cm}^{-3}$  has to be achieved, the Flibe spray temperature would have to be reduced to 783 K (50 K lower than the 833 K corresponding to this vapor density), with a slightly reduced spray flow rate requirement of  $2.3 \times 10^3$  kg/s. In either case, a small additional heat exchanger must

cool the spray flow. This heat exchanger would be used for feedwater heating.

The main Flibe flow entering the chamber will be a mixture of two streams with temperatures of 873 K from the steam generator (~20% of the flow) and 923 K from the recirculation loop (~80% of the flow). A small amount of cold Flibe could be sprayed into regions of the pocket shown in Fig. 3, in order to hold the vapor density below that corresponding to the temperature of the blanket. Future improvements in analysis of the central cavity pocket and venting phenomena will remove some of the unproven assumptions in the current spray system design; experiments will clearly be needed.

### III. NEUTRONICS AND ACTIVATION OF MATERIALS

The neutronics analysis of the HYLIFE-II reactor concept covers several areas<sup>29</sup> and includes the following:

1. calculating the number of tritons produced for each fusion reaction [i.e., the tritium breeding ratio (TBR)]
2. determining the energy released by nuclear reactions in the blanket, the target, and chamber structures from each fusion reaction. This energy is divided by 17.6 MeV to give the system energy multiplication factor (SEMF).
3. the energy deposition in the Flibe and FSW
4. the radiation damage rates measured by displacements per atom (dpa) and helium production.

The TBR is calculated to be 1.17. Nearly 15% of the tritium is bred in <sup>7</sup>Li, which makes up 92.4% of the natural lithium with the remainder being <sup>6</sup>Li. The SEMF is 1.18, bringing the 2100 MW of fusion power to almost 2500 MW(thermal).

The choice of a first-wall material for the chamber is not fully settled. The primary issues are compatibility with Flibe and minimization of the long-term activation for disposal considerations. The liquid curtain allows neutron wall damage to be a secondary issue.

Early in the study, low-activation Type 316 stainless steel was chosen as a structural material, in which manganese is substituted for nickel. This choice resulted in more decay heat (2.6-h half-life of <sup>56</sup>Mn) but less radioactivity on decommissioning for waste disposal. We discovered, however, that the manganese corrodes (dissolves) too readily in Flibe, and therefore, we chose the usual nickel-containing Type 316 stainless steel. Two candidate materials were considered for the FSW: Hastelloy and Type 316 stainless steel. The Type 316 stainless steel alloy is the one modified for use in fusion systems to reduce radiation-induced swelling and is called prime candidate alloy (PCA). The main differences are a somewhat higher nickel concentration (16% rather than 14%), a lower chromium concentration

(14% rather than 16.7%), and a small amount (~0.3%) of titanium. Results show that the Type 316 stainless steel is less expensive, is a superior choice for helium-generation-limited lifetime, has a longer dpa-limited lifetime, and has a lower shallow burial index (SBI). Hastelloy steels are superior in the areas of decay thermal power, corrosion resistance, and high-temperature strength.

The integrity of FSW materials under shutdown conditions (i.e., with no forced cooling) due to wall self-heating from activation product decay has been investigated. Calculations show this decay heat source is insufficient to melt the steel.

The main safety issue for HYLIFE-II is the requirement to contain almost all of the <sup>18</sup>F inventory (2-h half-life) to prevent its release to the public in case of a catastrophic accident (as discussed in Sec. V). Although fluorine itself is very chemically active, it is not volatile in the form of Flibe. Further, we find no energy source to cause a release of more than a few kilograms of Flibe. Therefore, special nuclear certification,<sup>42</sup> i.e., "N Stamp," with its attendant cost increases, is not needed for the Flibe activation products discussed here. Being able to build plant components to nonnuclear standards and codes would reduce the cost considerably.

Neutron radiation causes the properties of materials to degrade with time. One measure of this damage is the number of times each atom is displaced from its lattice site or dpa. Type 316 stainless steel retains its strength to ~100 dpa (Ref. 23). From Fig. 13, we see the dpa becomes 100 in 30 yr for a 0.56-m-thick liquid Flibe protection layer or a 1.6-m-thick liquid lithium

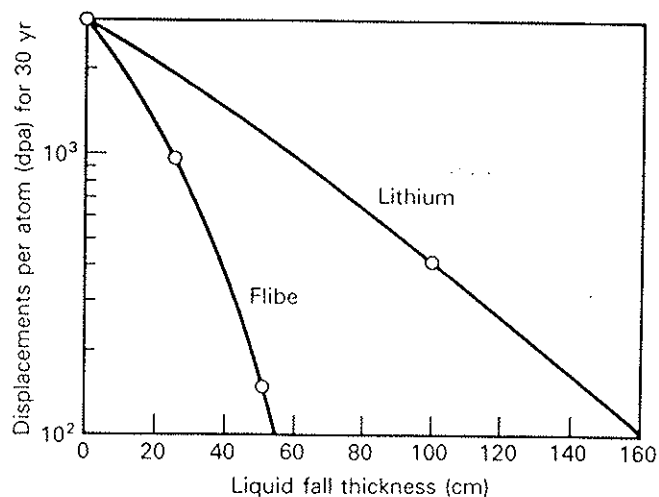


Fig. 13. Displacements per atom for 30 yr as a function of liquid fall thickness. A value of 100 dpa is an appropriate limit for Type 316 stainless steel.<sup>23</sup> In magnetic fusion designs, the 100-dpa limit is reached in only 2 yr. In 30 yr, there will be 1500 dpa (Ref. 23). The curves are based on calculations for 3-m radius, 2700-MW fusion power, and 80% capacity factor.

layer. (Without the protective liquid Flibe layer, the Type 316 stainless steel would reach 100 dpa in only ~1 yr.) A lifetime longer than 30 yr can easily be obtained by adding to the Flibe layer thickness.

The first wall is made of tubes that fail in a "soft" way, meaning that cracks that leak Flibe into the chamber are tolerable. The main structural wall, which must be vacuum tight, has an additional 500 mm of Flibe coolant between it and the FSW, which reduces radiation damage to insignificance. Similarly, the tips of the deflectors, which receive the most damage (100 dpa in 12 yr), can tolerate cracks because the stress there is the lowest.

A study of activation of the chamber was made to determine how much of the chamber would require deep burial on decommissioning.<sup>43</sup> With PCA, ~21% of the steel structure in the chamber design meets Class C requirements and thus can be disposed of by shallow burial; the SBI is <1. An increase of ~13 cm in Flibe shielding of the upper dome can increase this fraction to 42%. If the total structure is treated as one entity, its SBI is estimated to be 54. This could be reduced to 1.0 with an ~50-cm increase in effective Flibe shielding thickness overall.

The isotopes and their parents that dominate the SBI are <sup>94</sup>Nb (from niobium and molybdenum), <sup>99</sup>Tc (from molybdenum), and <sup>93</sup>Mo (from molybdenum), in that order. The order did not change over the range of Flibe thicknesses used. With 1 m of Flibe shielding, the SBIs from <sup>94</sup>Nb, <sup>99</sup>Tc, and <sup>93</sup>Mo are 11, 36, and 12, respectively, out of a total of 59. Since molybdenum and niobium activation dominate PCAs, we should strive to use materials without them. For example, a material such as Type 304 stainless steel (or Type 305 stainless steel) would reduce the SBI about two orders of magnitude to 0.72 compared with 54 for PCA when the structure is treated as a single entity. With Type 304 stainless steel, the isotopes and their likely parents that dominate the SBI are <sup>59</sup>Ni and <sup>63</sup>Ni (from nickel), and <sup>108m</sup>Ag (from silver). With 1 m of Flibe shielding, the SBIs from <sup>59</sup>Ni, <sup>63</sup>Ni, and <sup>108m</sup>Ag are 0.13, 0.26, and 0.15, respectively, out of a total of 0.55. Replacing some of the steel vessel components with graphite (carbon-carbon composites) could further reduce activation and the mass requiring deep burial.

#### IV. MATERIALS AND MOLTEN-SALT TECHNOLOGY

##### IV.A. Compatibility and Corrosion

For our vessel material and pipes, a Type 316 stainless steel will work with adequately low corrosion rates, and modified Hastelloy N (a high-nickel steel) will work even better. If the salt is kept reduced by keeping the mole fraction of tritium fluoride low enough, the corrosion rate of steel walls should be small (<2  $\mu\text{m}/\text{yr}$ ) (Ref. 44). The extracorrosive fluorine compounds and radicals formed during the evaporation process should

recombine before these compounds have a chance to react with the metal walls. The salt is reduced by contact with beryllium or the use of a buffering agent such as CeF<sub>3</sub> and CeF<sub>4</sub>.

In the future, we might consider the use of carbon-carbon composites for the vessel material because graphite is compatible with the molten salt and would be satisfactory if tritium retention is not too serious. Pyrolytic graphite has low retention, but porous forms of graphite have higher retention. The use of a Flibe-cooled graphite vessel will reduce activation, increase tritium breeding by reduced neutron absorption, and reduce heat leakage to the shield by absorbing neutrons more effectively.

##### IV.B. Chemical Kinetics of Dissociated Flibe

Some Flibe is ablated, vaporized, dissociated, and ionized into its constituents by X rays from the micro-explosion. These constituents will re-form Flibe and not other species because the chemical recombination to Flibe is strongly favored. Furthermore, based on a preliminary study, we believe that the recombination is sufficiently fast compared with time scales for the gas dynamics and condensation processes and that chemical equilibrium can be assumed for all gas dynamics and condensation processes. This permits the use of a recently developed equilibrium equation of state for Flibe vapor.<sup>45</sup>

Chemical recombination (e.g.,  $\text{Li} + \text{F} \rightarrow \text{LiF}$ ) will occur either by three-body collisions in the gas phase, or by heterogeneous recombination at liquid surfaces. Gas-phase recombination should dominate; Chen et al.<sup>24</sup> have predicted that all gas-phase chemical recombination processes are fast enough to maintain chemical equilibrium at pulse rates of 6 Hz and even much higher. Rapid condensation on droplet surfaces will require that the recombined constituents adhere and not bounce off when they strike the liquid. Too small an adherence ratio will slow condensation. We believe that LiF and BeF<sub>2</sub> (Flibe is a mixture of LiF and BeF<sub>2</sub>) will have a sticking coefficient close or equal to unity, and at least above 0.5 (Ref. 46). The binary composition of the vapor has the potential to introduce a diffusional resistance to condensation. However, at large condensation rates, this effect has been shown to be so small<sup>47</sup> that pure component behavior can be assumed. On the other hand, the presence of trace noncondensable species such as tritium and helium will affect condensation processes by creating a diffusional resistance. The areas of chemical kinetics and rapid condensation will require definitive experiments.

#### V. SAFETY AND ENVIRONMENT

An outstanding feature of the HYLIFE-II reactor is its favorable safety characteristics.<sup>48</sup> Safety and environmental goals for HYLIFE-II include the following:

1. For a plant with passive safety requirements, the off-site dose from a severe accident must be  $<2$  Sv (200 rem) so as to cause no immediate deaths.
2. The off-site dose in case of an accident involving components where no N stamp is required (i.e., "coal" standards can be used) must be  $<5$  mSv (0.5 rem). As discussed earlier, this goal may be overly restrictive (25 rem is a more customary criterion).
3. The dose from routine atmospheric effluents must be  $<50$   $\mu$ Sv/yr (5 mrem/yr).

To evaluate the potential to meet these goals, we studied the consequences of a severe accident involving chamber failure and breach of confinement, including the effects of activation products, tritium, and beryllium toxicity. According to fission reactor terminology, HYLIFE-II does not have a "containment" but rather a "confinement." (A containment is hermetically sealed and designed to contain the maximum credible pressure following an accident. A confinement is not hermetically sealed but vents in such a way as to minimize fission product release.)

In contrast to HYLIFE-I, with its flammable lithium inventory, the only large source of energy in the HYLIFE-II system available to disperse radioactive materials is the thermal energy of the molten Flibe. Because the secondary system uses water, it is credible that some water could collect in low points of the plant. A Flibe duct rupture injecting hundreds of kilograms of molten Flibe into a water pool has the potential to generate a steam explosion, which could breach the confinement and disperse some Flibe as a finely divided aerosol. Plant layout will be designed to avoid water anywhere near the Flibe ducts (except at the steam generator), thus minimizing the possibility of molten Flibe coming in direct contact with water. The double-walled-tube steam generators will have rupture disks to vent the steam pressure from the shell side in case of a double-tube rupture.

Another energy source is the microexplosion. Consideration was given to the possibility of radioisotope dispersion following a confinement breach during routine operations. The tritium inventory in the Flibe can be kept very low (below  $\sim 1$  g). The dominant activation product is  $\sim 300$  MCi of  $^{18}\text{F}$  (110-min half-life). A very small fraction ( $\sim 4 \times 10^{-6}$ ) of the Flibe activation products is mobilized under normal operation because the microexplosion vaporizes only  $\sim 10$  kg of the 2500 tonnes of Flibe. Only a fraction of the mobilized vapor would escape from a hole in the blast chamber, and only a fraction of that would leave from a hole in the confinement building. The  $^{18}\text{F}$  off-site dose from a severe accident (breaching both the blast chamber and the confinement and releasing 10 kg of Flibe aerosol) would be  $<0.2$  mSv (20 mrem).

Another possible accident would be a pipe break in which the tritium in the metal walls could be released

over a prolonged period of time. The estimated tritium inventory in the metal walls of the chamber and piping is 140 g, and in an accident, the off-site dose could be 13 mSv (1.3 rem). As discussed earlier, because this exceeds 5 mSv, nuclear-grade components were chosen for the vacuum disengager, piping, and chamber. These could be avoided if the tritium inventory in the walls were reduced by a factor of 3. With the cost of the chamber, pumps, and ducting estimated to be \$140 million for nuclear grade and \$93 million for coal standards, the savings would be considerable. The target factory will also be nuclear grade, but nuclear-grade components will probably not be required elsewhere. For example, the heavy-ion accelerator would not have to be nuclear grade.

Activation of metallic impurities in the Flibe from corrosion products or from target materials could result in high dose rates. As a result, contact maintenance is not feasible on the Flibe loop (unless a very effective impurity removal system were operating and activated impurities did not collect on pipe walls). Flibe leaks may pose a hazard for workers because beryllium compounds are toxic.

The routine effluent goal will be met provided the tritium removal system performs as predicted.

## VI. ECONOMIC ANALYSIS AND SYSTEMS ISSUES

The SAFIRE economics and systems analysis code was used to study some trends in HYLIFE-II (Ref. 32). For a constant plant power output, several cost contributions can be affected by pulse rate variation (and concomitant driver energy variation). As the pulse rate drops, the yield per shot must increase significantly to maintain power. To get a higher yield, the driver energy and the driver cost must go up, which adds dramatically to the total plant cost. As the pulse rate increases, the Flibe pumping power increases (the Flibe must be pumped faster to clear the chamber between shots and reestablish the pocket). The driver capital cost, however, decreases significantly with increasing pulse rate (smaller driver energy), so the net result is that the cost of electricity is a falling function of pulse rate up to  $\sim 10$  Hz or more. In future work, we plan to optimize the design by using parametric analysis.

Table III gives the cost breakdown for the two base cases for the latest HYLIFE-II unoptimized design. The basis for each cost item is given in the following references: Hoffman and Lee,<sup>17,19</sup> House,<sup>49</sup> and Longhurst and Dolan<sup>50</sup> for the reference point design at 1 GW(electric) and the enhanced 2-GW(electric) case given in Table I. The calculated COE for the 1-GW(electric) case is 6.5¢/kW·h in noninflated, constant 1990 dollars.

Figure 14 shows the dependence of the COE on driver cost, while Fig. 15 shows the dependence on power level. As Fig. 15 shows, reducing the net power



TABLE III  
Plant Cost Breakdown

Account	Item	Reference Case: 940 MW(electric) (millions 1990 dollars)		Enhanced Case: 1934 MW(electric) (millions 1990 dollars)	
		R + D + TF <sup>a</sup>	BOP	R + D + TF <sup>a</sup>	BOP
20	Land and land rights		11		11
21	Structures and improvements	58.3	70.9	88.5	100.2
22	Reactor plant equipment				
22.1	Reactor, bypass pumps, and pipe				
	Reactor	43.1		77.9	
	Bypass pumps	82.6		132.3	
	Bypass pipe	13.8		22.2	
22.2	Flibe coolant	102.6		165.0	
22.3	Vacuum system	5.4		6.3	
22.4	Target factory and equipment	51.4		59.5	
22.5	Tritium management system	92.0		127.8	
22.6	Shielding (in account 21)				
22.7	Heat transport system <sup>b</sup>				
	Coolant piping		10.9		18.2
	Coolant valves and bellows		19.1		31.8
	Pump and motors		37.1		61.8
	Coolant cleanup		15		25
	Steam separators		9.1		18.2
	Water loop piping		0.2		0.2
	Steam generators		36.9		68.9
22.8	Remote maintenance equipment	100		100	
23	Turbine plant equipment		178.1		313.4
24	Electric plant equipment		60.6		106.6
25	Miscellaneous plant equipment		23.7		41.7
26	Main heat rejection system		36.1		63.6
27	Driver equipment	570		680	
	Total direct cost	1119.2	508.7	1459.5	860.8
	Indirect cost factor	1.936	1.936	1.936	1.936
	Subtotal	2166.8	989.4	2825.6	1666.1
	Total capital cost		3151.6		4491.7
	Capital cost/kW(electric)		3353		2322
	COE <sup>c</sup> ( $\$/kW \cdot h$ )	3.4	1.5	2.1	1.3
	COE for O&M/SCR <sup>d</sup> /fuel	1.1	0.5	0.7	0.4
	Total COE		6.5		4.5

<sup>a</sup>Reactor + driver + target factory.

<sup>b</sup>There are three loops in the 1-GW(electric) case and five loops in the 2-GW(electric) case.

<sup>c</sup>The assumed availability was 75%; the capital rate for noninflating dollars was 9.66%.

<sup>d</sup>Scheduled component replacement and operations and maintenance (O&M) annually costed at 6% of direct cost.

to 500 MW(electric) has a major cost penalty, especially for the costly driver cases, whereas increasing the net power to  $\sim 2000$  MW(electric) has a major cost benefit and can reduce the COE to  $\sim 4.5\$/kW \cdot h$ .

The long lifetime of the liquid-protected walls and components in HYLIFE-II reduces the scheduled downtime for component replacement relative to a de-

sign without this protection. If the power plant availability were to increase from the assumed 75% to 85% (for example, 5 weeks less downtime per year by reduced changing of unprotected components as required in other reactor designs), the  $6.5\$/kW \cdot h$  would drop to  $5.7\$/kW \cdot h$ . If we also assume reduced scheduled component replacement (SCR) costs (i.e., no fuel rod

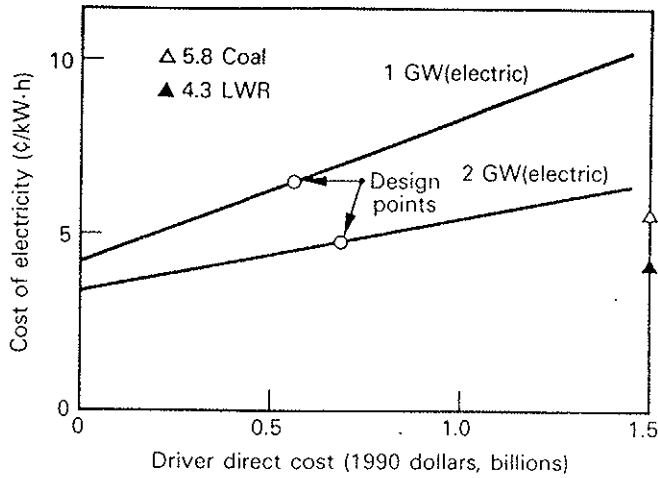


Fig. 14. The COE varies directly with driver cost. Driver cost is more important at 1 GW(electric) than at 2 GW(electric). At 1 GW(electric), drivers should cost much less than \$1 billion for IFE power plants in order to compete with future coal and nuclear costs.

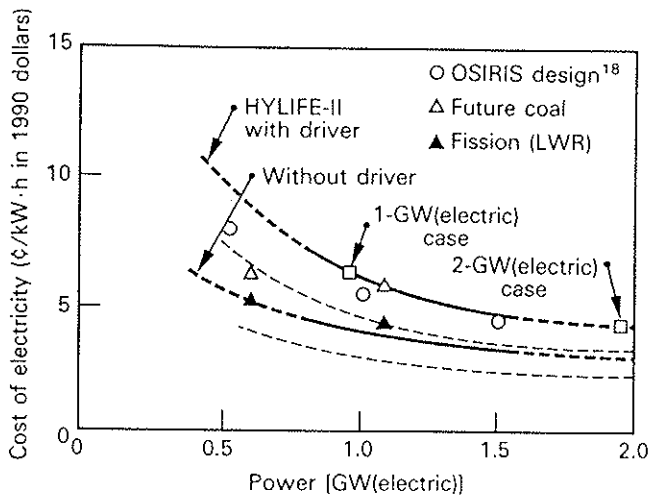


Fig. 15. Cost of electricity in constant 1990 dollars as a function of power. The importance of driver cost reduction and increasing plant size are shown. The driver cost assumed was \$570 million at 1 GW(electric) and \$680 million at 2 GW(electric). The dashed curves assume an availability of 85% and operations and maintenance and scheduled component replacement at 3% of direct cost, which might be appropriate to an IFE power plant with chamber wall protection such as HYLIFE-II (and assuming that the driver has low maintenance costs).

or first-wall replacement), such that the total operation and maintenance and SCR were 3% rather than 6%, the COE would drop to 5.0¢/kW·h for 1 GW(electric) and 3.9¢/kW·h for 2 GW(electric). The resulting lower

COE due directly to the wall protection concept is shown by the dashed curves in Fig. 15. The cost savings due to reduced downtime for the example given more than offsets the large cost of the additional Flibe and extra bypass pumps shown in Table III. The combined effects of higher availability and lower SCR costs made possible by HYLIFE-II's wall protection concept is such an important cost reduction that it deserves emphasis in future studies. Decommissioning costs were not considered in Table III but are expected to be small (~0.05¢/kW·h).

For comparison, the future coal power costs are predicted to be 5.8¢/kW·h at 1200 MW(electric) and 6.4¢/kW·h at 600 MW(electric), and the future LWR nuclear power costs are predicted to be 4.3¢/kW·h at 1200 MW(electric) and 5.2¢/kW·h at 600 MW(electric) in 1990 dollars.<sup>9</sup> When mined uranium becomes scarce and its cost increases from Delene's<sup>9</sup> assumed \$130/kg to, for example, \$300/kg, the cost of LWR electricity for fission plants would rise from 4.3 to 4.8¢/kW·h. Fusion might have to compete with the LWR fueled with either mined uranium or externally produced fuel or with the fission breeder, whichever is lower.

At this stage, however, cost estimates for IFE power plants are considered highly speculative. Further, just how much an IFE power plant can cost and still be acceptable and economically competitive in future years is unclear at this time. Other factors (e.g., safety, nonproliferation, and environmental aspects) will reflect on the future desirability of IFE, as well as its cost.

### VII. DEVELOPMENT PROGRAM REQUIRED

Many items requiring development for HYLIFE-II are also needed for any IFE plant and will only be noted briefly here: target design and performance, driver development, driver interface design, target injection, target tracking, and beam pointing.

The reason Flibe was chosen rather than liquid lithium was its safety advantages: It has orders of magnitude lower tritium inventory and no risk of water and air fires. Flibe, however, needs considerable development to enter industrial practice. Its advantages are probably worth the extra work that will be needed to bring our understanding from the point where the molten-salt reactor program left off ~20 yr ago.<sup>8</sup>

Some molten-salt items needing development effort are corrosion studies, cleanup systems (for small H<sub>2</sub>O leaks, corrosion product, and target material removal), and pump and valve development. Special valve design problems are posed by the reducing nature of salt. Oxides are stripped off metal surfaces, and self-welding of contacting metal parts occurs in a Flibe environment. The use of metal valves with a graphite seat is a likely development avenue. Freeze valves will need further development. Designs, however, should minimize the use of valves.

The large-capacity pumps (up to  $6.2 \text{ m}^3/\text{s}$ ) can be of conventional design but need development. Double-walled supercritical steam generators need development in, for example, construction methods, inspection, and plugging of failed tubes. Experimental confirmation of vacuum disengager performance is needed. Tests are needed on condensation to verify design assumptions. Experiments are needed to understand isochoric heating and gas venting to predict net outward momentum. Experiments and improved models are needed on evaporation due to target explosions and the resulting gas venting. The oscillating jets will need experimental development.

Further analysis and use of neutron test facilities will be needed to accurately predict neutron damage to the FSW. Ongoing work over many years will be needed for HYLIFE-II and fusion in general in order to design components so that the use of nuclear-grade components can be minimized. Work on future regulations should go hand-in-hand with design work. The standards used in coal-fired plants might be applicable for components whose failure does not result in harm to the public ( $<5\text{-mSv}$  off-site dose in case of an accident).

### VIII. SUMMARY AND CONCLUSIONS

In the design known as HYLIFE-II, we have modified the original HYLIFE design by substituting Flibe for lithium and increasing the pulse rate from 1.5 to 6 Hz. This was necessary to compensate for the vastly reduced target yields and gains predicted in recent studies. We developed an oscillating flow concept to allow this high pulse rate by reforming a pocket or central cavity in the Flibe jets quickly and still removing splash liquid from the beamlines before the next shot. Condensation is predicted to reduce the Flibe vapor pressure enough for beam propagation and still permit a 6-Hz pulse rate. The fire hazard of lithium has been eliminated, and safety requirements have been met (but shallow burial on decommissioning is not fully achieved).

At present, the design and performance of the system depend on many assumptions that must be verified by future analysis and experiment before we can have a high level of confidence in the predicted performance. Some of the key issues include verifying splash removal techniques, beam propagation, tritium removal effectiveness, condensation phenomena, and cost reduction. The heavy-ion driver and target factory have their own sets of unresolved issues not investigated here.

HYLIFE-II was estimated to be economically competitive with future coal power plants at a power level somewhat over 1 GW(electric) and with future fission power plants at a power at or somewhat under 2 GW(electric), although all cost calculations can only be considered very preliminary at this design level. To reduce the COE, we need a combination of driver cost

reduction and increased power plant size. Careful attention to safety might permit many components to be designed to coal power plant standards rather than nuclear power plant standards. Future work should emphasize lowering plant cost, always in the context of an integrated plant design.

### ACKNOWLEDGMENT

This work was performed under the auspices of the U.S. Department of Energy by Lawrence Livermore National Laboratory under contract W-7405-ENG-48.

### REFERENCES

1. J. A. BLINK, W. J. HOGAN, J. HOVINGH, W. R. MEIER, and J. H. PITTS, "The High-Yield Lithium-Injection Fusion-Energy (HYLIFE) Reactor," UCID-53559, Lawrence Livermore National Laboratory (1985).
2. R. J. BURKE et al., "Direct Conversion of Neutron Energy and Other Advantages of a Large Yield Per Pulse, Inertial-Confinement Fusion Reactor," ENG/CTR/TM-19, Argonne National Laboratory (1974).
3. W. SEIFRITZ and H. NAEGELE, "Uranium and Thorium Shells Serving as Tamers of D-T Fuel Pellets for Electron-Beam-Induced Fusion Approach," *Trans. Am. Nucl. Soc.*, **21**, 18 (1975).
4. M. MONSLER, J. MANISCALCO, J. BLINK, W. MEIER, and P. WALKER, "Electric Power from Laser Fusion: The HYLIFE Concept," *Proc. 13th Intersociety Energy Conversion Engineering Conf.*, San Diego, California, August 20-25, 1978; see also UCRL-1259, Lawrence Livermore National Laboratory (1978).
5. L. A. GLENN, "Transport Processes in an Inertial Confinement Fusion Reactor," *Nucl. Eng. Des.*, **64**, 375 (1981).
6. R. W. MOIR, M. G. ADAMSON, R. O. BANGERTER, R. L. BIERI, R. H. CONDIT, C. W. HARTMAN, P. A. HOUSE, A. B. LANGDON, B. G. LOGAN, C. D. ORTH, R. W. PETZOLDT, J. H. PITTS, J. H. POST, R. F. SACKS, M. T. TOBIN, W. H. WILLIAMS, T. J. DOLAN, G. R. LONGHURST, M. A. HOFFMAN, V. E. SCHROCK, P. F. PETERSON, R. Y. BAI, X. M. CHEN, J. LIU, D. K. SZE, and W. R. MEIER, "HYLIFE-II Progress Report," UCID-21816, Lawrence Livermore National Laboratory (1991).
7. R. W. MOIR, "HYLIFE-II Inertial Fusion Energy Power Plant Design," *Fusion Technol.*, **21**, 1475 (1992).
8. M. W. ROSENTHAL, P. N. HAUBENREICH, and R. B. BRIGGS, "The Development Status of Molten-Salt Breeder Reactors," ORNL-4812, Oak Ridge National Laboratory (1972).
9. J. G. DELENE, "Updated Comparison of Economics of Fusion Reactors," *Fusion Technol.*, **19**, 807 (1991).